Finite Elements in Analysis and Design 63 (2013) 42–50

Contents lists available at SciVerse ScienceDirect

Finite Elements in Analysis and Design

journal homepage: www.elsevier.com/locate/finel

Dynamic finite element analysis of axially vibrating nonlocal rods

S. Adhikari [a], T. Murmu [b,*], M.A. McCarthy [b]

[a] College of Engineering, Swansea University, Swansea SA2 8PP, UK
[b] Department of Mechanical, Aeronautical and Biomedical Engineering, Irish Centre for Composites Research, Materials and Surface Science Institute, University of Limerick, Ireland

ARTICLE INFO

Article history:
Received 9 March 2012
Received in revised form
31 May 2012
Accepted 7 August 2012

Keywords:
Axial vibration
Nonlocal mechanics
Dynamic stiffness
Asymptotic analysis
Frequency response

ABSTRACT

Free and forced axial vibrations of damped nonlocal rods are investigated. Two types of nonlocal damping models, namely, strain-rate-dependent viscous damping and velocity-dependent viscous damping, are considered. A frequency-dependent dynamic finite element method is developed to obtain the forced vibration response. Frequency-adaptive complex-valued shape functions are proposed to obtain the dynamic stiffness matrix in closed form. The stiffness and mass matrices of the nonlocal rod are also obtained using the conventional finite element method. Results from the dynamic finite element method and conventional finite element method are compared. Using an asymptotic analysis it is shown that, unlike its local counterpart, a nonlocal rod has a maximum cut-off frequency. A closed-form exact expression for this maximum frequency as a function of the nonlocal parameter has been obtained for undamped and damped systems. The frequency response function obtained using the proposed dynamic finite element method shows extremely high modal density near the maximum frequency. This leads to clustering of resonance peaks which is not easily obtainable using classical finite element analysis.

1. Introduction

Research on size-dependent structural theories for the accurate design and analysis of micro and nanostructures is growing rapidly [1–4]. This is because, though molecular dynamic (MD) simulation is justified for the analysis of nanostructures [5,6] such as nanorods, nanobeam, nanoplates, nanoshells and nanocones, the approach is computationally exorbitant for nanostructures with large numbers of atoms. This calls for the use of conventional continuum mechanics [7] and finite elements in analysis of nanostructures. However, classical continuum modelling approach is considered scale-free. It fails to account for the effects arising from the small-scale where size-effects are prominent.

Nanoscale experiments demonstrate that the mechanical properties of nano dimensional materials are much influenced by size effects or scale effects [8,9]. Size effects are related to atoms and molecules that constitute the materials. Further, atomistic simulations have also reported size effects on the magnitudes of resonance frequency and buckling load of nanoscale objects such as nanotubes and graphene [10,11]. The application of classical continuum approaches is thus questionable in the analysis of nanostructures such as nanorods, nanobeams and nanoplates. Examples of nanorods and nanobeams include carbon and boron nanotubes, while nanoplates can be graphene sheets or gold nanoplates.

One widely promising size-dependant continuum theory is the nonlocal elasticity theory pioneered in [12] which brings in the scale effects and underlying physics within the formulation. Nonlocal elasticity theory contains information related to the forces between atoms, and the internal length scale in structural, thermal and mechanical analyses. In the nonlocal elasticity theory, the small-scale effects are captured by assuming that the stress at a point is a function of the strains at all points in the domain. Nonlocal theory considers long-range inter-atomic interaction and yields results dependent on the size of a body [12]. Some drawbacks of classical continuum theory can be efficiently avoided and the size-dependent phenomena can be reasonably explained by nonlocal elasticity. Recent literature shows that the theory of nonlocal elasticity is being increasingly used for reliable and fast analysis of nanostructures. Studies include nonlocal analysis of nanostructures viz. nanobeams [13–15], nanoplates [16], carbon nanotubes [17], graphene [18], microtubules [19] and nanorings [20].

Recently due to elevated interests in nanotechnology, various one-dimensional nanostructures have been realised. They include nanorods, nanowires, nanobelts, nanotubes, nanobridges, nanonails, nanowalls and nanohelixes. Among all the one-dimensional nanostructures, nanotubes, nanorods and nanowires are the most widely studied. This is because of the easy material formation and device applications. One important one-dimensional

* Corresponding author. Tel.: +353 61 202253; fax: +353 61 202944.
E-mail address: murmutony@gmail.com (T. Murmu).

0168-874X/$ - see front matter © 2012 Elsevier B.V. All rights reserved.
http://dx.doi.org/10.1016/j.finel.2012.08.001

nanostructure is nanorods. Nanorods [21] are one-dimensional objects ranging from 1 to 3000 nm in length. They can be grown from various methods, including (i) vapour phase synthesis [22], (ii) metal-organic chemical vapour deposition [23], (iii) hydrothermal synthesis [24]. Nanorods have found application in a variety of nanodevices, including ultraviolet photodetectors, nanosensors, transistors, diodes and LED arrays.

Axial vibration experiments can be used for the determination of the Youngs modulus of Carbon Nanotubes (CNTs). Generally, the flexural modes occur at low frequencies. However vibrating nanobeams (CNTs) may also have longitudinal modes at relatively high frequencies and can be of very practical significance in high operating frequencies. Nanorods when used as electromechanical resonators can be externally excited and exhibit axial vibrations. Furthermore for a moving nanoparticle inside a single-walled carbon nanotube (SWCNT), the SWCNT generally vibrates both in the transverse and longitudinal directions. The longitudinal vibration is generated because of the friction existing between the outer surface of the moving nanoparticle and the inner surface of the SWCNT. It is also reported [25] that transport measurements on suspended SWCNTs show signatures of phonon-assisted tunnelling, influenced by longitudinal vibration (stretching) modes. Chowdhury et al. [26] have reported sliding axial modes for multiwalled carbon nanotubes (MWCNTs). Tong et. al [27] have considered axial buckling of MWCNTs with heterogeneous boundary conditions.

Only limited work on nonlocal elasticity has been devoted to the axial vibration of nanorods. Aydogdu [28]developed a nonlocal elastic rod model and applied it to investigate the small scale effect on the axial vibration of clamped-clamped and clamped-free nanorods. Filiz and Aydogdu [29] applied the axial vibration of nonlocal rod theory to carbon nanotube heterojunction systems. Narendra and Gopalkrishnan [30] have studied the wave propagation of nonlocal nanorods. Recently Murmu and Adhikari [31] have studied the axial vibration analysis of a double-nanorod-system. In this paper, we will be referring to a nanorod as a nonlocal rod, so as to distinguish it from a local rod.

Several computational techniques have been used for solving the nonlocal governing differential equations. These techniques include Naviers Method [32], Differential Quadrature Method (DQM) [33] and the Galerkin technique [34]. Recently attempts have been made to develop a Finite Element Method (FEM) based on nonlocal elasticity. The upgraded finite element method in contrast to other methods above can effectively handle more complex geometry, material properties as well as boundary and/or loading conditions. Pisano et al. [35] reported a finite element procedure for nonlocal integral elasticity. Recently some motivating work on a finite element approach based on nonlocal elasticity was reported [36]. The majority of the reported works consider free vibration studies where the effect of non-locality on the eigensolutions has been studied. However, forced vibration response analysis of nonlocal systems has received very little attention.

Based on the above discussion, in this paper we develop the dynamic finite element method based on nonlocal elasticity with the aim of considering dynamic response analysis. The dynamic finite element method belongs to the general class of spectral methods for linear dynamical systems [37]. This approach, or approaches very similar to this, is known by various names such as the dynamic stiffness method [38–48], spectral finite element method [37,49] and dynamic finite element method [50,51]. Some of the key features of the method are:

- The mass distribution of the element is treated in an exact manner in deriving the element dynamic stiffness matrix.
- The dynamic stiffness matrix of one-dimensional structural elements, taking into account the effects of flexure, torsion, axial and shear deformation, and damping, is exactly determinable, which, in turn, enables the exact vibration analysis by an inversion of the global dynamic stiffness matrix.
- The method does not employ eigenfunction expansions and, consequently, a major step of the traditional finite element analysis, namely, the determination of natural frequencies and mode shapes, is eliminated which automatically avoids the errors due to series truncation.
- Since modal expansion is not employed, ad hoc assumptions concerning the damping matrix being proportional to the mass and/or stiffness are not necessary.
- The method is essentially a frequency-domain approach suitable for steady state harmonic or stationary random excitation problems.
- The static stiffness matrix and the consistent mass matrix appear as the first two terms in the Taylor expansion of the dynamic stiffness matrix in the frequency parameter.

So far the dynamic finite element method has been applied to classical local systems only. In this paper we generalise this approach to nonlocal systems. One of the novel features of the analysis proposed here is the employment of frequency-dependent complex nonlocal shape functions for damped systems. This in turn enables us to obtain the element stiffness matrix using the usual weak form of the finite element method.

The paper is organised as follows. In Section 2 we introduce the equation of motion of axial vibration of undamped and damped rods. Natural frequencies and their asymptotic behaviours for both cases are discussed for different boundary conditions. The conventional and the dynamic finite element method are developed in Section 3. Closed form expressions are derived for the mass and stiffness matrices. In Section 4 the proposed methodology is applied to an armchair single walled carbon nanotube (SWCNT) for illustration. Theoretical results, including the asymptotic behaviours of the natural frequencies, are numerically illustrated. Finally, in Section 5 some conclusions are drawn based on the results obtained in the paper.

2. Axial vibration of damped nonlocal rods

2.1. Equation of motion

The equation of motion of axial vibration for a damped nonlocal rod can be expressed as

$$EA\frac{\partial^2 U(x,t)}{\partial x^2}+\widehat{c}_1\left(1-(e_0a)_1^2\frac{\partial^2}{\partial x^2}\right)\frac{\partial^3 U(x,t)}{\partial x^2 \partial t} =\widehat{c}_2\left(1-(e_0a)_2^2\frac{\partial^2}{\partial x^2}\right)\frac{\partial U(x,t)}{\partial t}+\left(1-(e_0a)^2\frac{\partial^2}{\partial x^2}\right) \times\left\{m\frac{\partial^2 U(x,t)}{\partial t^2}+F(x,t)\right\} \tag{1}$$

This is an extension of the equation of motion of an undamped nonlocal rod for axial vibration [28,31,52]. Here EA is the axial rigidity, m is the mass per unit length, e_0a is the nonlocal parameter [12], $U(x,t)$ is the axial displacement, $F(x,t)$ is the applied force, x is the spatial variable and t is the time. The constant $\widehat{c}_1$ is the strain-rate-dependent viscous damping coefficient and $\widehat{c}_2$ is the velocity-dependent viscous damping coefficient. The parameters $(e_0a)_1$ and $(e_0a)_2$ are nonlocal parameters related to the two damping terms respectively. For simplicity we have not taken into account any nonlocal effect related to the damping. Although this can be mathematically incorporated in the analysis, the determination of these nonlocal parameters is beyond the scope of this work and therefore only local interaction for the damping is adopted. Thus, in the following analysis we consider $(e_0a)_1=(e_0a)_2=0$. Assuming harmonic response as

$$U(x,t)=u(x)\exp[\mathrm{i}\omega t] \tag{2}$$

and considering free vibration, from Eq. (1) we have

$$\left(1+\mathrm{i}\omega\frac{\widehat{c}_1}{EA}-\frac{m\omega^2}{EA}(e_0a)^2\right)\frac{d^2u}{dx^2}+\left(\frac{m\omega^2}{EA}-\mathrm{i}\omega\frac{\widehat{c}_2}{EA}\right)u(x)=0 \tag{3}$$

Following the damping convention in dynamic analysis [53], we consider stiffness and mass proportional damping. Therefore, we express the damping constants as

$$\widehat{c}_1=\zeta_1(EA) \quad \text{and} \quad \widehat{c}_2=\zeta_2(m) \tag{4}$$

where ζ_1 and ζ_2 are stiffness and mass proportional damping factors. Substituting these, from Eq. (3) we have

$$\frac{d^2u}{dx^2}+\alpha^2u=0 \tag{5}$$

where

$$\alpha^2=\frac{(\omega^2-\mathrm{i}\zeta_2\omega)/c^2}{(1+\mathrm{i}\omega\zeta_1-(e_0a)^2\omega^2/c^2)} \tag{6}$$

with

$$c^2=\frac{EA}{m} \tag{7}$$

It can be noticed that α^2 is a complex function of the frequency parameter ω. In the special case of undamped systems when damping coefficients ζ_1 and ζ_1 go to zero, α^2 in Eq. (6) reduces to $\Omega^2/(1-(e_0a)^2\Omega^2)$, which is a real function of ω.

2.2. Analysis of damped natural frequencies

Natural frequencies of undamped nonlocal rods have been discussed in the literature [28]. Natural frequencies of damped systems receive little attention. The damped natural frequency depends on the boundary conditions. We denote a parameter σ_k as

$$\sigma_k=\frac{k\pi}{L} \quad \text{for clamped-clamped boundary conditions} \tag{8}$$

$$\text{and } \sigma_k=\frac{(2k-1)\pi}{2L} \quad \text{for clamped-free boundary conditions} \tag{9}$$

Following the conventional approach [53], the natural frequencies can be obtained from

$$\alpha=\sigma_k \tag{10}$$

Taking the square of this equation and denoting the natural frequencies as ω_k we have

$$(\omega_k^2-\mathrm{i}\zeta_2\omega_k)=\sigma_k^2c^2(1+\mathrm{i}\omega_k\zeta_1-(e_0a)^2\omega_k^2/c^2) \tag{11}$$

Rearranging we obtain

$$\omega_k^2(1+\sigma_k^2(e_0a)^2)-\mathrm{i}\omega_k(\zeta_2+\zeta_1\sigma_k^2c^2)-\sigma_k^2c^2=0 \tag{12}$$

This is a very generic equation and many special cases can be obtained from this as follows:

- *Undamped local systems:* This case can be obtained by substituting $\zeta_1=\zeta_2=0$ and $e_0a=0$. From Eq. (12) we therefore obtain

  $$\omega_k=\sigma_kc \tag{13}$$

  which is the classical expression [53].
- *Undamped nonlocal systems:* This case can be obtained by substituting $\zeta_1=\zeta_2=0$. Solving Eq. (12) we therefore obtain

  $$\omega_k=\frac{\sigma_kc}{\sqrt{1+\sigma_k^2(e_0a)^2}} \tag{14}$$

  which is obtained in [28].
- *Damped local systems:* This case can be obtained by substituting $\zeta_1=\zeta_2=0$. Solving Eq. (12) we obtain

  $$\omega_k=\mathrm{i}(\zeta_2+\zeta_1\sigma_k^2c^2)/2\pm\sigma_kc\sqrt{1-(\zeta_1\sigma_kc+\zeta_2/(\sigma_kc))^2/4} \tag{15}$$

  Therefore, the decay rate is $(\zeta_2+\zeta_1\sigma_k^2c^2)/2$ and damped oscillation frequency is $\sigma_kc\sqrt{1-(\zeta_1\sigma_kc+\zeta_2/(\sigma_kc))^2/4}$. We observe that damping effectively reduces the oscillation frequency.

For the general case of a nonlocal damped system, the damped frequency can be obtained by solving Eq. (12) as

$$\omega_k=\frac{\mathrm{i}(\zeta_2+\zeta_1\sigma_k^2c^2)}{2(1+\sigma_k^2(e_0a)^2)}\pm\frac{\sigma_kc}{\sqrt{1+\sigma_k^2(e_0a)^2}}\sqrt{1-\frac{(\zeta_1\sigma_kc+\zeta_2/(\sigma_kc))^2}{4(1+\sigma_k^2(e_0a)^2)}} \tag{16}$$

Therefore, the decay rate is given by $(\zeta_2+\zeta_1\sigma_k^2c^2)/2(1+\sigma_k^2(e_0a)^2)$ and the damped oscillation frequency is given by

$$\omega_{d_k}=\frac{\sigma_kc}{\sqrt{1+\sigma_k^2(e_0a)^2}}\sqrt{1-\frac{(\zeta_1\sigma_kc+\zeta_2/(\sigma_kc))^2}{4(1+\sigma_k^2(e_0a)^2)}} \tag{17}$$

It can be observed that the nonlocal damped system has the lowest natural frequencies. Note that the expressions derived here are general in terms of the boundary conditions.

2.3. Asymptotic analysis of natural frequencies

In this paper we are interested in dynamic response analysis of damped nonlocal rods. As a result, behaviour of the natural frequencies across a wide frequency range is of interest. An asymptotic analysis is conducted here to understand the frequency behaviour in the high frequency limit. We first consider the undamped natural frequency given by Eq. (14). To obtain asymptotic values, we rewrite the frequency equation in (14) and take the mathematical limit $k\to\infty$ to obtain

$$\lim_{k\to\infty}\omega_k=\lim_{k\to\infty}\frac{c}{\sqrt{\frac{1}{\sigma_k^2}+(e_0a)^2}}=\frac{c}{(e_0a)}=\frac{1}{(e_0a)}\sqrt{\frac{EA}{m}} \tag{18}$$

This is obtained by noting the fact that for $k\to\infty$, for both sets of boundary conditions we have $\sigma_k\to\infty$. The result in Eq. (18) shows that there exists an 'upper limit' of frequency in nonlocal systems. This upper limit of frequency is an inherent property of a nonlocal system. It is a function of material properties only and independent of the boundary conditions and the length of the rod. The smaller the value of e_0a, the larger this upper limit becomes. Eventually for a local system $e_0a=0$ and the upper limit becomes infinite, which is well known.

Now we turn our attention to the oscillation frequency of the damped system. Rewriting the expressions for the oscillation frequency from Eq. (17) and taking the limit as $k\to\infty$ we obtain

$$\lim_{k\to\infty}\omega_{d_k}=\lim_{k\to\infty}\frac{c}{\sqrt{\frac{1}{\sigma_k^2}+(e_0a)^2}}\sqrt{1-\frac{\left(\zeta_1c+\frac{1}{\sigma_k^2}(\zeta_2/c)\right)^2}{4\left(\frac{1}{\sigma_k^2}+(e_0a)^2\right)}}$$
$$=\frac{c}{(e_0a)}\sqrt{1-\left(\frac{\zeta_1c}{2e_0a}\right)^2} \tag{19}$$

Therefore the upper frequency limit for the damped systems is lower than that of the undamped system. It is interesting note that it is independent of the mass proportional damping ζ_2. Only the stiffness proportional damping has an effect on the upper frequency limit. Eq. (19) can also be used to obtain an asymptotic critical damping factor. For vibration to continue, the term within the square root in Eq. (19) must be greater than zero. Therefore, the asymptotic critical damping factor for nonlocal rods can be obtained as

$$(\zeta_1)_{\text{crit}} = \frac{2e_0 a}{c} \tag{20}$$

In practical terms this implies that the value of ζ_1 should be less than this value for high frequency vibration. Again observe that like the upper frequency limit, the asymptotic critical damping factor is a function of material properties only and independent of the boundary conditions and the length of the rod.

The spacing between the natural frequencies is important for dynamic response analysis as the shape of the frequency response function depends on the spacing. Because k is an index, the derivative $d\omega_k/dk$ is not meaningful as k is an integer. However, in the limit $k\to\infty$, we can obtain mathematically $d\omega_k/dk$ and it would mean the rate of change of frequencies with respect to the counting measure. This in turn is directly related to the frequency spacing. For the local rod it is well known that frequencies are uniformly spaced. This can be seen by differentiating ω_k in Eq. (13) as

$$\lim_{k\to\infty} \frac{d\omega_k}{dk} = c\frac{d\sigma_k}{dk} \quad \text{where} \quad \frac{d\sigma_k}{dk} = \frac{\pi}{L} \tag{21}$$

for both sets of boundary conditions. For nonlocal rods, from Eq. (14) we have

$$\lim_{k\to\infty} \frac{d\omega_k}{dk} = \lim_{k\to\infty} \frac{d}{dk}\left(\frac{c}{\sqrt{\frac{1}{\sigma_k^2} + (e_0 a)^2}} \right) = \lim_{k\to\infty} \frac{\pi}{L} \frac{c}{\left(\frac{1}{\sigma_k^2} + (e_0 a)^2 \right)^{3/2} \sigma_k^2}$$
$$= \lim_{k\to\infty} \frac{\pi}{L} \frac{c}{(e_0 a)^3} \frac{1}{\sigma_k^2} = 0 \tag{22}$$

The limit in the preceding equation goes to zero because $\sigma_k \to \infty$ for $k\to\infty$. This shows that unlike local systems, for large values of k, the undamped natural frequencies of nonlocal rods will tend to cluster together. A similar conclusion can be drawn by considering the damped natural frequencies also. Next we consider classical and dynamic finite element methods for dynamic response calculations.

3. Dynamic finite element matrix

3.1. Classical finite element of nonlocal rods

We first consider standard finite element analysis of the nonlocal rod. Recently Phadikar and Pradhan [36] proposed a variational-formulation-based finite element approach for nanobeams and nanoplates. Let us consider an element of length L with axial stiffness EA and mass per unit length m. An element for the damped axially vibrating rod is shown in Fig. 1. This element has two degrees of freedom and there are two shape functions $N_1(x)$ and $N_2(x)$. The shape function matrix for the axial deformation can be given by [54]

$$\mathbf{N}(x) = [N_1(x), N_2(x)]^T = [1 - x/L, x/L]^T \tag{23}$$

Using this the stiffness matrix can be obtained using the conventional variational formulation as

$$\mathbf{K}_e = EA \int_0^L \frac{d\mathbf{N}(x)}{dx}\frac{d\mathbf{N}^T(x)}{dx}\,\mathrm{d}x = \frac{EA}{L}\begin{bmatrix} 1 & -1 \\ -1 & 1 \end{bmatrix} \tag{24}$$

Fig. 1. An element for the axially vibrating rod with damping. The axial rigidity AE and mass per unit length m are assumed to be uniform along the length. The element has two degrees of freedom and the displacement field within the element is complex and frequency dependent.

The mass matrix for the nonlocal element can be obtained as

$$\mathbf{M}_e = m\int_0^L \mathbf{N}(x)\mathbf{N}^T(x)\,\mathrm{d}x + m(e_0 a)^2 \int_0^L \frac{d\mathbf{N}(x)}{dx}\frac{d\mathbf{N}^T(x)}{dx}\,\mathrm{d}x$$
$$= \frac{mL}{6}\begin{bmatrix} 2 & 1 \\ 1 & 2 \end{bmatrix} + mL(e_0 a/L)^2 \begin{bmatrix} 1 & -1 \\ -1 & 1 \end{bmatrix}$$
$$= mL\begin{bmatrix} 1/3 + (e_0 a/L)^2 & 1/6 - (e_0 a/L)^2 \\ 1/6 - (e_0 a/L)^2 & 1/3 + (e_0 a/L)^2 \end{bmatrix} \tag{25}$$

For the special case when the rod is local, the mass matrix derived above reduces to the classical mass matrix as $e_0 a = 0$.

3.2. Dynamic finite element for damped nonlocal rod

The first step for the derivation of the dynamic element matrix is the generation of dynamic shape functions. The dynamic shape functions are obtained such that the equation of dynamic equilibrium is satisfied exactly at all points within the element. Similar to the classical finite element method, assume that the frequency-dependent displacement within an element is interpolated from the nodal displacements as

$$u_e(x,\omega) = \mathbf{N}^T(x,\omega)\hat{\mathbf{u}}_e(\omega) \tag{26}$$

Here $\hat{\mathbf{u}}_e(\omega) \in \mathbb{C}^n$ is the nodal displacement vector $\mathbf{N}(x,\omega) \in \mathbb{C}^n$ is the vector of frequency-dependent shape functions and $n = 2$ is the number of the nodal degrees-of-freedom. Suppose the $s_j(x,\omega) \in \mathbb{C}, j = 1,2$ are the basis functions which exactly satisfy Eq. (5). It can be shown that the shape function vector can be expressed as

$$\mathbf{N}(x,\omega) = \mathbf{\Gamma}(\omega)\mathbf{s}(x,\omega) \tag{27}$$

where the vector $\mathbf{s}(x,\omega) = \{s_j(x,\omega)\}^T, \forall j = 1,2$ and the complex matrix $\mathbf{\Gamma}(\omega) \in \mathbb{C}^{2\times 2}$ depends on the boundary conditions.

In order to obtain $\mathbf{s}(x,\omega)$ first assume that

$$u(x) = \overline{u}\,\exp[kx] \tag{28}$$

where k is the wave number. Substituting this in Eq. (5) we have

$$k^2 + \alpha^2 = 0 \quad \text{or} \quad k = \pm \mathrm{i}\alpha \tag{29}$$

In view of the solutions in Eq. (29), the complex displacement field within the element can be expressed by a linear combination of the basis functions $e^{-\mathrm{i}\alpha x}$ and $e^{\mathrm{i}\alpha x}$ so that in our notations $\mathbf{s}(x,\omega) = \{e^{-\mathrm{i}\alpha x}, e^{\mathrm{i}\alpha x}\}^T$. Therefore, it is more convenient to express $\mathbf{s}(x,\omega)$ in terms of trigonometric functions. Considering $e^{\pm \mathrm{i}\alpha x} = \cos(\alpha x) \pm \mathrm{i}\sin(\alpha x)$, the vector $\mathbf{s}(x,\omega)$ can be alternatively expressed as

$$\mathbf{s}(x,\omega) = \begin{Bmatrix} \sin(\alpha x) \\ \cos(\alpha x) \end{Bmatrix} \in \mathbb{C}^2 \tag{30}$$

Considering unit axial displacement boundary condition as $u_e(x = 0,\omega) = 1$ and $u_e(x = L,\omega) = 1$, after some elementary algebra, the shape function vector can be expressed in the form of Eq. (27) as

$$\mathbf{N}(x,\omega) = \mathbf{\Gamma}(\omega)\mathbf{s}(x,\omega) \quad \text{where } \mathbf{\Gamma}(\omega) = \begin{bmatrix} -\cot(\alpha L) & 1 \\ \operatorname{cosec}(\alpha L) & 0 \end{bmatrix} \in \mathbb{C}^{2\times 2} \tag{31}$$

Simplifying this we obtain the dynamic shape functions as

$$\mathbf{N}(x,\omega)=\begin{bmatrix}-\cot(\alpha L)\sin(\alpha x)+\cos(\alpha x)\\ \operatorname{cosec}(\alpha L)\sin(\alpha x)\end{bmatrix} \tag{32}$$

Taking the limit as ω goes to 0 (that is the static case) it can be shown that the shape function matrix in Eq. (32) reduces to the classical shape function matrix given by Eq. (23). Therefore the shape functions given by Eq. (32) can be viewed as the generalisation of the nonlocal dynamical case.

The stiffness and mass matrices can be obtained similarly to the static finite element case discussed before. Note that for this case all the matrices become complex and frequency-dependent. It is more convenient to define the dynamic stiffness matrix as

$$\mathbf{D}_e(\omega)=\mathbf{K}_e(\omega)-\omega^2\mathbf{M}_e(\omega) \tag{33}$$

so that the equation of dynamic equilibrium is

$$\mathbf{D}_e(\omega)\widehat{\mathbf{u}}_e(\omega)=\widehat{\mathbf{f}}(\omega) \tag{34}$$

In Eq. (33), the frequency-dependent stiffness and mass matrices can be obtained as

$$\mathbf{K}_e(\omega)=EA\int_0^L \frac{d\mathbf{N}(x,\omega)}{dx}\frac{d\mathbf{N}^T(x,\omega)}{dx}\,\mathrm{d}x$$

$$\text{and}\quad \mathbf{M}_e(\omega)=m\int_0^L \mathbf{N}(x,\omega)\mathbf{N}^T(x,\omega)\,\mathrm{d}x \tag{35}$$

After some algebraic simplifications [46,55] it can be shown that the dynamic stiffness matrix is given by the following closed-form expression

$$\mathbf{D}_e(\omega)=EA\alpha\begin{bmatrix}\cot(\alpha L) & -\operatorname{cosec}(\alpha L)\\ \operatorname{cosec}(\alpha L) & \cot(\alpha L)\end{bmatrix} \tag{36}$$

This is in general a 2×2 matrix with complex entries. The frequency response of the system at the nodal point can be obtained by simply solving Eq. (34) for all frequency values. The calculation only involves inverting a 2×2 complex matrix and the results are exact with only one element for any frequency value. This is a significant advantage of the proposed dynamic finite element approach compared to the conventional finite element approach discussed in the pervious subsection.

So far we did not explicitly consider any forces within the element. A distributed body force can be considered following the usual finite element approach [54] and replacing the static shape functions with the dynamic shape functions (32). Suppose $p_e(x,\omega)$, $x\in[0,L]$ is the frequency-depended distributed body force. The element nodal forcing vector can be obtained as

$$\mathbf{f}_e(\omega)=\int_0^L p_e(x,\omega)\mathbf{N}(x,\omega)\,\mathrm{d}x \tag{37}$$

As an example, if a point harmonic force of magnitude p is applied at length $b<L$ then, $p_e(x,\omega)=p\delta(x-b)$ where $\delta(\bullet)$ is the Dirac delta function. The element nodal force vector becomes

$$\mathbf{f}_e(\omega)=p\int_0^L \delta(x-b)\mathbf{N}(x,\omega)\,\mathrm{d}x=p\begin{Bmatrix}-\cot(\alpha L)\sin(\alpha b)+\cos(\alpha b)\\ \operatorname{cosec}(\alpha L)\sin(\alpha b)\end{Bmatrix} \tag{38}$$

Next we illustrate the formulation derived in this section using an example.

4. Numerical results and discussions

We consider an SWCNT to illustrate the theory developed in this paper. An armchair (5, 5) SWCNT with Young's modulus E=6.85 TPa, L=25 nm, density $\rho=9.517\times 10^3$ kg/m^3 and thickness t=0.08 nm is considered as in [56]. We consider only mass proportional damping such that the damping factor $\zeta_2=0.05$ and $\zeta_1=0$. By comparing with MD simulation results [10,6] it was observed that $e_0a=1$ nm is the optimal value of the nonlocal parameter. In this study however we consider a range of values of e_0a within 0–2 nm to understand its role in the dynamic response. Although the role of the nonlocal parameter on the natural frequencies has been investigated, its effect on the dynamic response is relatively unknown. It is assumed that the SWCNT is fixed at one end and we are interested in the frequency response at the free end due to harmonic excitation. Using the dynamic finite element approach only one 'finite element' is necessary as the equation of motion is solved exactly. We consider natural frequencies and dynamic response of the CNT due to a harmonic force at the free edge.

First we look into the nature of the novel nonlocal dynamic shape functions employed in this study. In Fig. 2 the amplitudes of the two dynamic shape functions as a function of frequency for $e_0a=0.5$ nm are shown. For convenience, the shape functions are plotted against normalised frequency

$$\widehat{\omega}=\omega/\omega_{1l} \tag{39}$$

and normalised length coordinate x/L. Here ω_{1l} is the first natural frequency of the local rod [53], given by

$$\omega_{1l}=\frac{\pi}{2L}\sqrt{\frac{EA}{m}} \tag{40}$$

Similar plots for $e_0a=2.0$ nm are shown in Fig. 3 to examine the influence of the nonlocal parameter on the dynamic shape

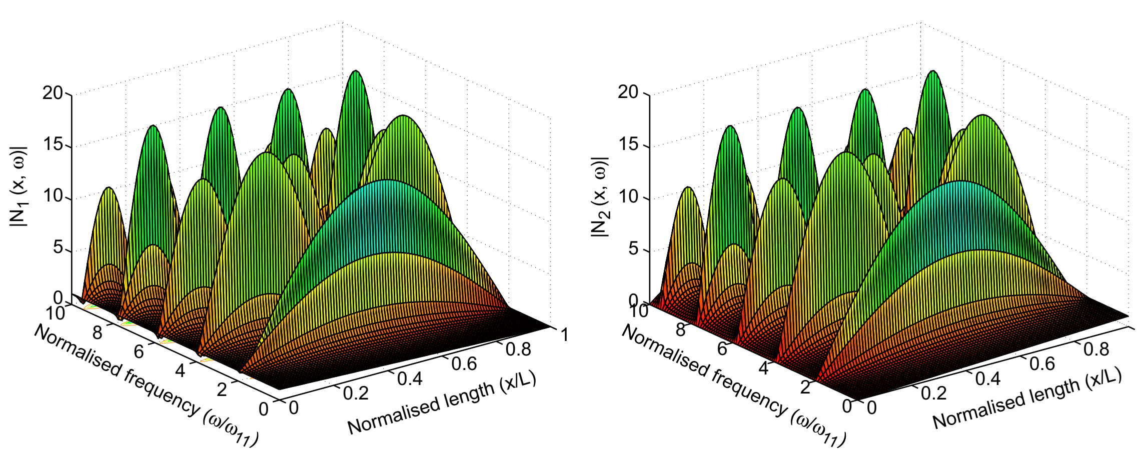

Fig. 2. Amplitude of the dynamic shape functions as a function of frequency for $e_0a=0.5$ nm. (a) Shape function $N_1(x,\omega)$ and (b) shape function $N_2(x,\omega)$.

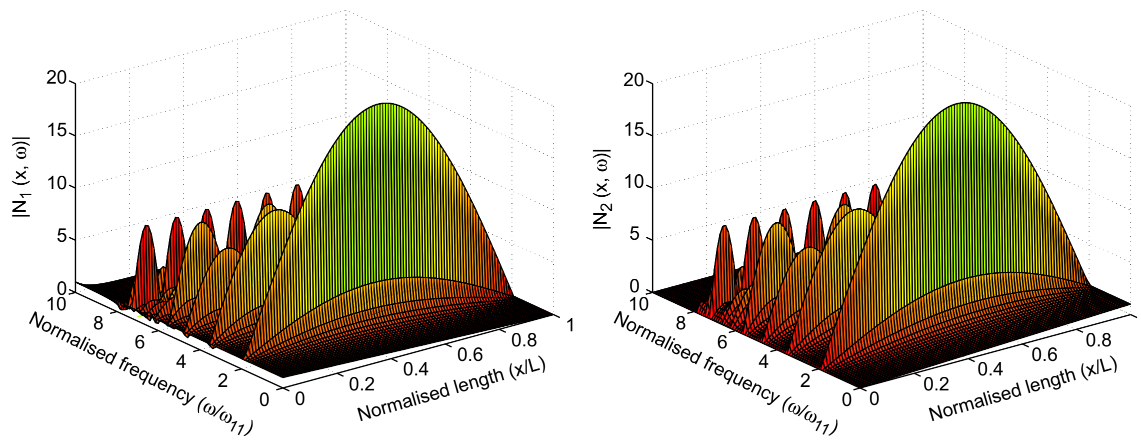

Fig. 3. Amplitude of the dynamic shape functions as a function of frequency for $e_0a = 2.0$ nm. (a) Shape function $N_1(x,\omega)$ and (b) shape function $N_2(x,\omega)$.

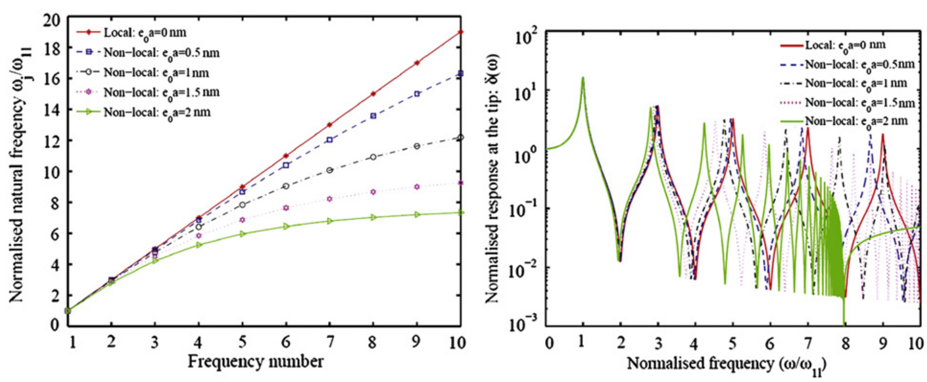

Fig. 4. The variation of undamped natural frequency and dynamic response for different values of e_0a. The local case along with four representative values of e_0a is considered. (a) Normalised undamped natural frequency (ω_j/ω_{1l}) and (b) normalised dynamic frequency response amplitude.

functions. The plots of the shape functions show the following interesting features:

- At zero frequency (that is for the static case) the shape functions reduce to the classical linear functions given by Eq. (23). It can be observed that $N_1(0,0)=1$, $N_2(L,0)=0$ and $N_2(0,0)=0$, $N_2(L,0)=1$.
- For increasing frequency, the shape functions become nonlinear in x and adapt themselves according to the vibration modes. One can observe multiple modes in the higher frequency range. This nonlinearity in the shape functions is the key for obtaining the exact dynamic response using the proposed approach.
- Figs. 2 and 3 also show the role of the nonlocal parameter. In Fig. 3 one can observe more number of modes in the high frequency range. This is due to the fact that natural frequency of the nonlocal rod reduced with the increase in the value of the nonlocal parameter.

The shape functions used for the proposed dynamic finite element analysis do not give the natural frequencies directly. By considering the undamped system (that is by substituting $\zeta_2=0$ and $\zeta_1=0$ in Eq. (6)), setting the denominator of any of the shape functions to zero, and solving the resulting equation one can obtain the natural frequencies. Following this, from Eq. (32) one has $\sin(\alpha L)=0$. This in turn will give an expression identical to the frequency equation in (14). In Fig. 4, the first 10 normalised natural frequencies and the normalised displacement amplitude of the dynamic response at the tip of the SWCNT are shown. The normalised displacement amplitude is defined by

$$\delta(\omega) = \frac{\widehat{u}_2(\omega)}{u_{\text{static}}} \tag{41}$$

where u_{static} is the static response at the free edge given by $u_{\text{static}} = FL/EA$. Assuming the amplitude of the harmonic excitation at the free edge is F, the dynamic response can be obtained using the equation of dynamic equilibrium (34) as

$$\widehat{u}_2(\omega) = \frac{F}{EA\alpha\cot(\alpha L)} = \frac{F\tan(\alpha L)}{EA\alpha} \tag{42}$$

Therefore, the normalised displacement amplitude in Eq. (41) is given by

$$\delta(\omega) = \frac{\widehat{u}_2(\omega)}{u_{\text{static}}} = \left(\frac{F\tan(\alpha L)}{EA\alpha}\right) \Big/ (FL/EA) = \frac{\tan(\alpha L)}{\alpha L} \tag{43}$$

The frequency axis of the response amplitude in Fig. 4(b) is normalised similarly to the plots of the shape functions given earlier. The frequency plot in Fig. 4(a) clearly shows that the natural frequencies decrease with increasing value of the nonlocal parameter e_0a. One interesting feature arising for larger values of e_0a is that the frequency curve effectively becomes 'flat'. This implies that the natural frequencies reach a terminal value as shown by the asymptotic analysis in Section 2.3. Using Eq. (18), for large values of k, the normalised natural frequency plotted in Fig. 4(a) would approach to

$$\frac{\omega_k}{\omega_{1l}} \approx \frac{2/\pi}{(e_0a/L)} \tag{44}$$

Therefore, for $e_0a = 2$ nm, we have $\omega_{k\max} \le 7.957$. Clearly, the smaller the value of e_0a, the larger this upper limit becomes.

The consequence of this upper limit can be seen in the frequency response amplitude plot in Fig. 4(b). For higher values e_0a, more and more resonance peaks are clustered within a frequency band. Indeed in Eq. (22) we have proved that asymptotically, the spacing between the natural frequencies goes to zero. This implies that higher natural frequencies of a nonlocal system are very closely spaced. In Fig. 4(b), this fact can be observed in the frequency band $7 \lesssim \widehat{\omega} \lesssim 8$ for the case when $e_0a = 2$ nm. The same behaviour is expected for other values of e_0a in the higher frequency ranges. It is worth pointing out that the frequency response curve for the case of $e_0a = 2.0$ nm is invalid after $\widehat{\omega} > 8$ as it is beyond the maximum frequency limit. From Fig. 4(b) it can also be seen that the resonance peak shifts to the left for increasing values of e_0a. This shift corresponds to the reduction in the natural frequencies as shown in Fig. 4(a).

Now we compare the results from the dynamic finite element and conventional finite element methods. The natural frequencies can be obtained using the nonlocal finite element method developed in Section 3.1. By assembling the element stiffness and mass matrices given by Eqs. (24) and (25) and solving the resulting matrix eigenvalue problem $\mathbf{K}\boldsymbol{\phi}_j = \omega_j^2 \mathbf{M}\boldsymbol{\phi}_j, j = 1,2,\ldots$ one can obtain the both the eigenvalues and eigenvectors (denoted by $\boldsymbol{\phi}_j$ here). For the numerical calculation we used 100 elements. This in turn, results in global mass and stiffness matrices of dimension 200×200. In Fig. 5, the natural frequencies obtained from the nonlocal finite element method are compared with the analytical expression in Eq. (14) for four values of e_0a within the range of 0.5–2.0 nm. Excellent agreement was found for the first ten natural frequencies. However, the results become quite different for the dynamic response as shown in Fig. 6. In the numerical calculations, 10^5 points are used in the frequency axis. The frequency response functions from the standard finite element were obtained using the classical modal series method [53]. For small values of e_0a the results from the dynamic finite element and standard finite element method agree well, as seen in Fig. 6(a) and (b). The discrepancies between the methods increase for higher values of e_0a as seen in Fig. 6(c) and (d). Note that the results from the dynamic finite element approach are exact as it does not suffer from error arising due to finite element discretisation. For higher values of e_0a, increasing numbers of natural frequencies lie within a given frequency range. As a result a very fine mesh is necessary to capture the high number of modes. If the given frequency is close the maximum cutoff frequency derived in (18), then a very high number of finite elements will be necessary (theoretically infinitely many and there exist an infinite number of frequencies up to the cut off frequency). In such a situation effectively the conventional finite element analysis breaks down, as seen in Fig. 6(d) in the range $7 \leq \widehat{\omega} < 8$. The proposed dynamic finite element is effective in these situations as it does not suffer from discretisation errors as in the conventional finite element method.

5. Conclusions

In this paper a novel dynamic finite element approach for axial vibration of damped nonlocal rods is proposed. Strain rate dependent viscous damping and velocity dependent viscous damping are considered. Damped and undamped natural frequencies for general boundary conditions are derived. An asymptotic analysis is used to understand the behaviour of the frequencies and their spacings in the high-frequency limit. Frequency dependent complex-valued shape functions are used to obtain the dynamic stiffness matrix in closed form. The dynamic response in the frequency domain can be obtained by inverting the dynamic stiffness matrix. The stiffness and mass matrices of the nonlocal rod were also obtained using the conventional finite element method. In the special case when the nonlocal parameter

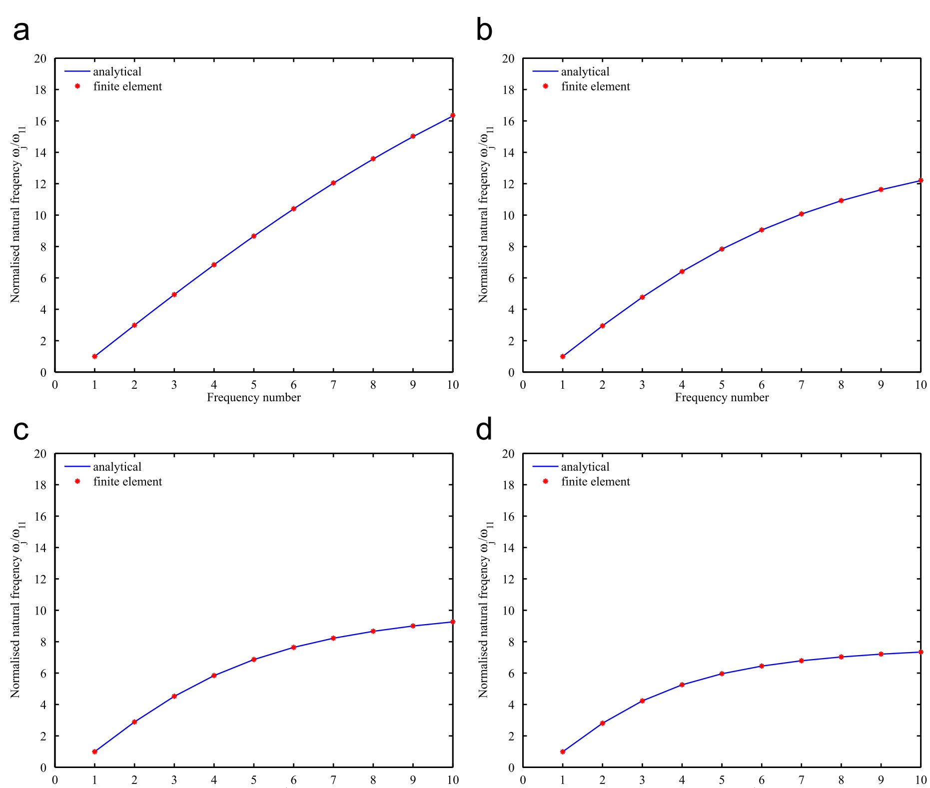

Fig. 5. Normalised natural frequency (ω_j/ω_{1l}) at the tip for different values of e_0a. Analytical results are compared with the finite element (with 100 elements) results. (a) $e_0a = 0.5$ nm, (b) $e_0a = 1.0$ nm, (c) $e_0a = 1.5$ nm and (d) $e_0a = 2.0$ nm.

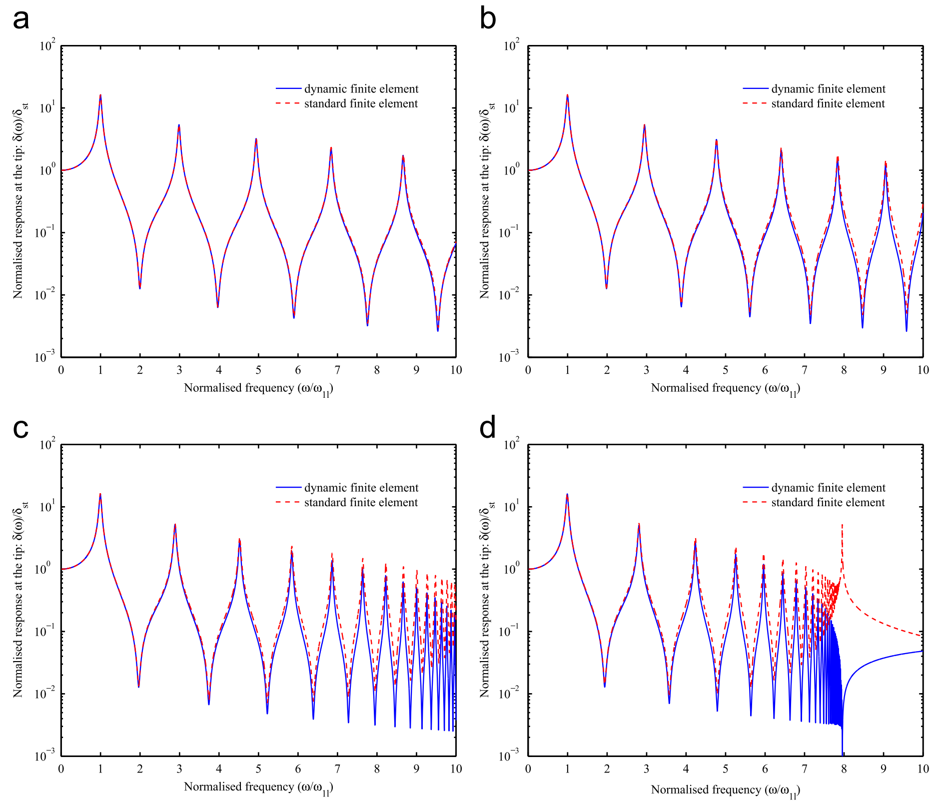

Fig. 6. Amplitude of the normalised dynamic frequency response at the tip for different values of e_0a. Dynamic finite element results (with one element) is compared with the conventional finite element results (with 100 elements). (a) $e_0a = 0.5$ nm, (b) $e_0a = 1.0$ nm, (c) $e_0a = 1.5$ nm and (d) $e_0a = 2.0$ nm.

becomes zero, the expression of the mass matrix reduces to the classical case. The proposed method is numerically applied to the axial vibration of a (5,5) carbon nanotube. Some of the key contributions made in this study are:

- Unlike local rods, nonlocal rods have an upper cut-off natural frequency. Using an asymptotic analysis, it was shown that for an undamped rod, the natural frequency $(\omega_{k_{max}}) \to (1/(e_0a))\sqrt{EA/m}$. This maximum frequency does not depend on the boundary conditions or the length of the rod.
- Near to the maximum frequency, the spacing between the natural frequencies becomes very small. This in turn leads to clustering of the resonance peaks near the maximum frequency.
- For the oscillation frequency of damped systems, the upper cut-off frequency is given by $(\omega_{k_{max}}) \to (c/(e_0a))\sqrt{1-(\zeta_1 c/2e_0a)^2}$ where $c=\sqrt{EA/m}$ and ζ_1 is the stiffness proportional damping factor arising from the strain rate dependent viscous damping constant. The velocity dependent viscous damping has no affect on the maximum frequency of the damped rod.
- The asymptotic critical damping factor for nonlocal rods is given by $(\zeta_1)_{crit} = 2e_0a\sqrt{m/EA}$.

The natural frequencies and the dynamic response obtained using the conventional finite element approach were compared with the results obtained using the dynamic finite method. Good agreement between the two methods was found for small values of the nonlocal parameter. For larger values of the nonlocal parameter, the conventional finite element approach is unable to capture the dynamics due to very high modal density near to the maximum frequency. In this case the proposed dynamic finite element approach provides a simple and robust alternative.

Acknowledgments

S.A. acknowledges the support of Royal Society of London through the award of Wolfson Research Merit award. TM acknowledges the support from the Irish Research Council for Science, Engineering & Technology (IRCSET).

References

[1] B. Akgoz, O. Civalek, Strain gradient elasticity and modified couple stress models for buckling analysis of axially loaded micro-scaled beams, Int. J. Eng. Sci. 49 (11) (2011) 1268–1280.
[2] M.H. Kahrobaiyan, M. Asghari, M. Rahaeifard, M. Ahmadian, Investigation of the size-dependent dynamic characteristics of atomic force microscope microcantilevers based on the modified couple stress theory, Int. J. Eng. Sci. 48 (12) (2010) 1985–1994.
[3] S. Kong, S. Zhou, Z. Nie, K. Wang, Static and dynamic analysis of micro beams based on strain gradient elasticity theory, Int. J. Eng. Sci. 47 (4) (2009) 487–498.
[4] P. Chhapadia, P. Mohammadi, P. Sharma, Curvature-dependent surface energy and implications for nanostructures, J. Mech. Phys. Solids 59 (10) (2011) 2103–2115.
[5] R. Chowdhury, S. Adhikari, F. Scarpa, M.I. Friswell, Transverse vibration of single layer graphene sheets, J. Phys. D: Appl. Phys. 44 (20) (2011) 205401:1–205401:11.
[6] R. Chowdhury, S. Adhikari, C.Y. Wang, F. Scarpa, A molecular mechanics approach for the vibration of single walled carbon nanotubes, Comput. Mater. Sci. 48 (4) (2010) 730–735.
[7] V.L. Berdichevsky, Theory of elastic plates and shells, in: Variational Principles of Continuum Mechanics II: Applications, Interaction of Mechanics and Mathematics, Springer, 2009.
[8] Y.H. Zhao, Y.Z. Guo, Q. Wei, T.D. Topping, A.M. Dangelewicz, Y.T. Zhu, T.G. Langdon, E.J. Lavernia, Influence of specimen dimensions and strain measurement methods on tensile stress–strain curves, Mater. Sci. Eng. A Struct. Mater. Prop. Microstructure Process. 525 (1–2) (2009) 68–77.
[9] J. Biener, A.M. Hodge, J.R. Hayes, C.A. Volkert, L.A. Zepeda-Ruiz, A.V. Hamza, F.F. Abraham, Size effects on the mechanical behaviour of nanoporous au, Nano Lett. 6 (10) (2006) 2379–2382.

[10] R. Chowdhury, S. Adhikari, F. Scarpa, Vibrational analysis of zno nanotubes: A molecular mechanics approach, Appl. Phys. A 102 (2) (2011) 301–308.
[11] F. Scarpa, S. Adhikari, A mechanical equivalence for the Poisson's ratio and thickness of C–C bonds in single wall carbon nanotubes, J. Phys. D: Appl. Phys. 41 (085306) (2008) 1–5.
[12] A. Eringen, On differential-equations of nonlocal elasticity and solutions of screw dislocation and surface waves, J. Appl. Phys. 54 (9) (1983) 4703–4710.
[13] A. Pisano, P. Fuschi, Closed form solution for a nonlocal elastic bar in tension, Int. J. Solids Struct. 40 (1) (2003) 13–23.
[14] Y.Y. Zhang, C.M. Wang, N. Challamel, Bending, buckling, and vibration of micro/nanobeams by hybrid nonlocal beam model, J. Eng. Mech. ASCE 136 (5) (2010) 562–574.
[15] P. Lu, H.P. Lee, C. Lu, P.Q. Zhang, Application of nonlocal beam models for carbon nanotubes, Int. J. Solids Struct. 44 (16) (2007) 5289–5300.
[16] K. Kiani, Small-scale effect on the vibration of thin nanoplates subjected to a moving nanoparticle via nonlocal continuum theory, J. Sound Vib. 330 (20) (2011) 4896–4914.
[17] P. Karaoglu, M. Aydogdu, On the forced vibration of carbon nanotubes via a non-local Euler–Bernoulli beam model, Proc. Inst. Mech. Eng. Part C J. Mech. Eng. Sci. 224 (C2) (2010) 497–503.
[18] A.T. Samaei, S. Abbasion, M.M. Mirsayar, Buckling analysis of a single-layer graphene sheet embedded in an elastic medium based on nonlocal Mindlin plate theory, Mech. Res. Commun. 38 (7) (2011) 481–485.
[19] O. Civalek, C. Demir, Bending analysis of microtubules using nonlocal Euler–Bernoulli beam theory, Appl. Math. Modelling 35 (5) (2011) 2053–2067.
[20] C.M. Wang, W.H. Duan, Free vibration of nanorings/arches based on nonlocal elasticity, J. Appl. Phys. 104 (2008) 014303.
[21] J. Wen, J. Lao, D. Wang, T. Kyaw, Y. Foo, Z. Ren, Self-assembly of semiconducting oxide nanowires, nanorods, and nanoribbons, Chem. Phys. Lett. 372 (5–6) (2003) 717–722.
[22] A.N. Red'kin, Z.I. Makovei, A.N. Gruzintsev, S.V. Dubonos, E.E. Yakimov, Vapor phase synthesis of aligned zno nanorod arrays from elements, Inorg. Mater. 43 (3) (2007) 253–257.
[23] W. Park, D. Kim, S. Jung, G. Yi, Metalorganic vapor-phase epitaxial growth of vertically well-aligned zno nanorods, Appl. Phys. Lett. 80 (22) (2002) 4232–4234.
[24] J. Choy, E. Jang, J. Won, J. Chung, D. Jang, Y. Kim, Hydrothermal route to zno nanocoral reefs and nanofibers, Appl. Phys. Lett. 84 (2) (2004) 287–289.
[25] S. Sapmaz, P. Jarillo-Herrero, Y. Blanter, C. Dekker, H. van der Zant, Tunneling in suspended carbon nanotubes assisted by longitudinal phonons, Phys. Rev. Lett. 96(2).
[26] R. Chowdhury, C.Y. Wang, S. Adhikari, F.M. Tong, Sliding oscillations of multiwall carbon nanotubes, Phys. E Low-dimensional Syst. Nanostruct. 42 (9) (2010) 2295–2300.
[27] F.M. Tong, C.Y. Wang, S. Adhikari, Axial buckling of multiwall carbon nanotubes with heterogeneous boundary conditions, J. Appl. Phys. 105 (2009) 094325:1–094325:7.
[28] M. Aydogdu, Axial vibration of the nanorods with the nonlocal continuum rod model, Physica E 41 (5) (2009) 861–864.
[29] S. Filiz, M. Aydogdu, Axial vibration of carbon nanotube heterojunctions using nonlocal elasticity, Comput. Mater. Sci. 49 (3) (2010) 619–627.
[30] S. Narendar, S. Gopalakrishnan, Non local scale effects on ultrasonic wave characteristics nanorods, Phys. E Low-Dimensional Syst. Nanostruct. 42 (5) (2010) 1601–1604.
[31] T. Murmu, S. Adhikari, Nonlocal effects in the longitudinal vibration of double-nanorod systems, Phys. E: Low-dimensional Syst. Nanostruct. 43 (1) (2010) 415–422.
[32] S.C. Pradhan, Buckling of single layer graphene sheet based on nonlocal elasticity and higher order shear deformation theory, Phys. Lett. A 373 (45) (2009) 4182–4188.
[33] P. Malekzadeh, A.R. Setoodeh, A.A. Beni, Small scale effect on the free vibration of orthotropic arbitrary straight-sided quadrilateral nanoplates, Compos. Struct. 93 (7) (2011) 1631–1639.
[34] R.D. Firouz-Abadi, M.M. Fotouhi, H. Haddadpour, Free vibration analysis of nanocones using a nonlocal continuum model, Phys. Lett. A 375 (41) (2011) 3593–3598.
[35] A.A. Pisano, A. Sofi, P. Fuschi, Nonlocal integral elasticity: 2d finite element based solutions, Int. J. Solids Struct. 46 (21) (2009) 3836–3849.
[36] J.K. Phadikar, S.C. Pradhan, Variational formulation and finite element analysis for nonlocal elastic nanobeams and nanoplates, Comput. Mater. Sci. 49 (3) (2010) 492–499.
[37] J.F. Doyle, Wave Propagation in Structures, Springer Verlag, New York, 1989.
[38] M. Paz, Structural Dynamics: Theory and Computation, 2nd Ed., Van Nostrand, Reinhold, 1980.
[39] J.R. Banerjee, F.W. Williams, Exact Bernoulli–Euler dynamic stiffness matrix for a range of tapered beams, Int. J. Numer. Methods Eng. 21 (12) (1985) 2289–2302.
[40] J.R. Banerjee, Coupled bending torsional dynamic stiffness matrix for beam elements, Int. J. Numer. Methods Eng. 28 (6) (1989) 1283–1298.
[41] J.R. Banerjee, F.W. Williams, Coupled bending-torsional dynamic stiffness matrix for Timoshenko beam elements, Comput. Struct. 42 (3) (1992) 301–310.
[42] J.R. Banerjee, S.A. Fisher, Coupled bending torsional dynamic stiffness matrix for axially loaded beam elements, Int. J. Numer. Methods Eng. 33 (4) (1992) 739–751.
[43] N.J. Ferguson, W.D. Pilkey, Literature review of variants of dynamic stiffness method, Part 1: the dynamic element method, Shock Vib. Dig. 25 (2) (1993) 3–12.
[44] N.J. Ferguson, W.D. Pilkey, Literature review of variants of dynamic stiffness method, part 2: frequency-dependent matrix and other, Shock Vib. Dig. 25 (4) (1993) 3–10.
[45] J.R. Banerjee, F.W. Williams, Free-vibration of composite beams—an exact method using symbolic computation, J. Aircraft 32 (3) (1995) 636–642.
[46] C.S. Manohar, S. Adhikari, Dynamic stiffness of randomly parametered beams, Probabilistic Eng. Mech. 13 (1) (1998) 39–51.
[47] J.R. Banerjee, Dynamic stiffness formulation for structural elements: a general approach, Comput. Struct. 63 (1) (1997) 101–103.
[48] S. Adhikari, C.S. Manohar, Transient dynamics of stochastically parametered beams, ASCE J. Eng. Mech. 126 (11) (2000) 1131–1140.
[49] S. Gopalakrishnan, A. Chakraborty, D.R. Mahapatra, Spectral Finite Element Method, Springer Verlag, New York, 2007.
[50] S.M. Hashemi, M.J. Richard, G. Dhatt, A new Dynamic Finite Element (DFE) formulation for lateral free vibrations of Euler–Bernoulli spinning beams using trigonometric shape functions, J. Sound Vib. 220 (4) (1999) 601–624.
[51] S.M. Hashemi, M.J. Richard, Free vibrational analysis of axially loaded bending-torsion coupled beams: a dynamic finite element, Comput. Struct. 77 (6) (2000) 711–724.
[52] J.N. Reddy, Nonlocal theories for bending, buckling and vibration of beams, Int. J. Eng. Sci. 45 (2–8) (2007) 288–307.
[53] L. Meirovitch, Principles and Techniques of Vibrations, Prentice-Hall International, Inc., New Jersey, 1997.
[54] M. Petyt, Introduction to Finite Element Vibration Analysis, Cambridge University Press, Cambridge, UK, 1998.
[55] S. Adhikari, Doubly spectral stochastic finite element method (DSSFEM) for structural dynamics, ASCE J. Aerosp. Eng. 24 (3) (2011) 264–276.
[56] T. Murmu, S. Adhikari, Nonlocal vibration of carbon nanotubes with attached buckyballs at tip, Mech. Res. Commun. 38 (1) (2011) 62–67.